Applied Physics Letters

Modulation of current-time traces by two-pore arrangements of polyimide nanofluidic diodes

Cite as: Appl. Phys. Lett. **115**, 183701 (2019); https://doi.org/10.1063/1.5125042
Submitted: 20 August 2019 . Accepted: 17 October 2019 . Published Online: 30 October 2019

Patricio Ramirez, Javier Cervera, Vicente Gomez, Mubarak Ali, Saima Nasir, Wolfgang Ensinger, and Salvador Mafe

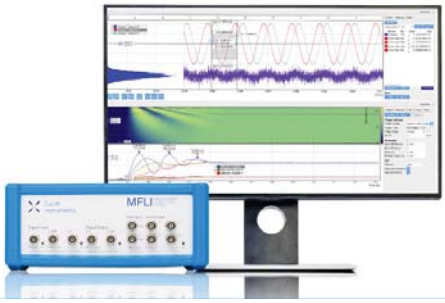

Applied Physics Letters ARTICLE scitation.org/journal/apl

Modulation of current-time traces by two-pore arrangements of polyimide nanofluidic diodes

Cite as: Appl. Phys. Lett. **115**, 183701 (2019); doi: 10.1063/1.5125042
Submitted: 20 August 2019 · Accepted: 17 October 2019 ·
Published Online: 30 October 2019

Patricio Ramirez,[1,a)] Javier Cervera,[2] Vicente Gomez,[1] Mubarak Ali,[3,4] Saima Nasir,[3,4] Wolfgang Ensinger,[4] and Salvador Mafe[2]

AFFILIATIONS

[1]Dept. de Física Aplicada, Univ. Politècnica de València, E-46022 Valencia, Spain
[2]Dept. de Física de la Terra i Termodinàmica, Universitat de València, E-46100 Burjassot, Spain
[3]Materials Research Department, GSI Helmholtzzentrum für Schwerionenforschung, Planckstrasse 1, D-64291 Darmstadt, Germany
[4]Department of Material- and Geo-Sciences, Materials Analysis, Technische Universität Darmstadt, Alarich-Weiss-Straße 2, D-64287 Darmstadt, Germany

[a)]**Electronic mail:** patraho@fis.upv.es

ABSTRACT

Liquid state arrangements of two polymeric membranes with single conical nanopores constitute nanofluidic diodes that allow a rich electrical functionality based on the modulation of individual conductances in aqueous electrolyte solutions. In particular, the prescribed sequences of current-time traces can be obtained by preprogramed switching between series and parallel pore connection arrangements. Hybrid nanopore-solid-state circuits are also possible. The basic applied physics of the nanofluidic diode arrangements can be understood from simple circuit theory concepts and should be of widespread interest to sensing and actuating procedures, controlled release dispensers, and energy conversion modules based on electrochemical signals.

We have studied different arrangements of two polymeric membranes with single conical nanopores that behave as externally tunable nanofluidic diodes in electrolyte solutions. The pore physical chemistry does not involve exceedingly difficult nor highly specific surface functionalization, and inward and outward rectifications can be obtained.[1–5] The motivation for this research is twofold: (*i*) the surface charge-regulated ionic transport at nanoscale volumes involves fundamental principles of applied physics and (*ii*) this subject is of widespread interest to sensing and actuating procedures, controlled release dispensers, and energy conversion modules based on electrochemical signals. Note, in particular, that ionic circuits of nanopores can operate in aqueous solutions, and thus, these nanostructures may allow information processing in physiological environments.[1,4–6]

The experimental data presented herein show that the physics of two-pore arrangements including nanofluidic diodes can be useful to closely related disciplines such as applied analytical chemistry, biomedical engineering, and energy storage. Because we have demonstrated that the physical concepts used are sound and their implementation is feasible, the results can provide opportunities for electrochemical signal processing based on the individual modulation of nanofluidic conductances.[1–6]

The experimental characteristics of the single conical nanopores and the measuring electrochemical cell have been given elsewhere.[2,7] The pores are obtained by single-ion irradiation of 12.5-μm thick polyimide (PI) foils (Kapton50 HN, DuPont) at the linear accelerator UNILAC (GSI, Darmstadt). After irradiation, asymmetric track-etching converts the membrane tracks into approximately conically shaped pores[8,9] whose radii are in the ranges of 10–60 nm (tip) and 300–800 nm (base).[7] The ionization of the carboxylate residues obtained by track-etching gives a negative charge on the pore surface at neutral pH values in aqueous salt solutions.[7,9] The absolute values of the surface charge density are in the range of 0.1–1.0 e/nm^2, where e is the elementary charge.[2,7,9] The conical geometry provides a spatially inhomogenous axial distribution of charge that makes the pore behave as a nanofluidic diode.[7,9]

We used different sets of pores, but only the results obtained with two samples were finally included. The pores used in this study had the following characteristics: Surface charge density $\sigma = 1$ e/nm^2, pore base radius $a_b = 500$ nm, and pore tip radius $a_t = 20$ nm for sample 1; $\sigma = 0.8$ e/nm^2, $a_b = 400$ nm, and $a_t = 9$ nm for sample 2. The opening radii and surface charges were determined as follows. First, the pore base radius was obtained by field emission scanning electron

microscopy using a multipore sample that was etched simultaneously with the single-pore sample. Second, the pore tip radius was obtained from the experimental single pore I–V curves at acidic pH (neutral pore). Using these pore radii, the only free parameter in a Poisson–Nernst–Planck theoretical model discussed elsewhere[10] is the surface pore charge density, which can be determined from the experimental I–V curve.

The experimental characteristics of arrangements composed of two single-pore nanofluidic diodes mounted in their electrochemical cells were reproducible across all the measurements, with typical current deviations lower than 5% for each individual pore. The experimental reproducibility of the I–V curves and pore rectification ratios has been studied in detail previously.[7,10] Ag|AgCl electrodes are dipped into 0.1 M KCl aqueous solutions to control the input potentials and output currents using a Keithley 6487 picoammeter (Keithley Instruments, Cleveland, Ohio).[7] The current (I)–voltage (V) curves are characterized by high resistances at $V < 0$ (the current enters the cone base of the negatively charged pore) and low resistances at $V > 0$ (the current enters the cone tip).[10] The nanofluidic diodes require a spatially asymmetric charge distribution[1–3,7–9] of sufficiently high surface charge density $\sigma = 0.1$–$1\ e/\mathrm{nm}^2$, together with bathing electrolyte concentrations around 0.1 M,[10] to achieve significant rectification ratios. The pH effects are also relevant: The pores show negative charges at neutral pH values, while they are positively charged at acidic pH values,[7] although specific functionalization can modify this operating pH range.[1,2,4–6]

Figure 1(a) shows the setup and the different electrical responses [Figs. 1(b)–1(f)] due to the distinct conductance regimes and current rectifications that are obtained with the series and parallel connections (*insets*). The I–V curves are obtained with pore samples 1 and 2. These pores are arranged as individual nanofluidic diodes in opposite orientations [Fig. 1(b)] and in series and parallel connections with the diodes either in the same or in opposite orientations [Figs. 1(c)–1(f)]. The current is dominated by conductive rather than by capacitive phenomena because of the relatively slow electric signals employed.[2,7,10] The wide range of electrochemical responses (Fig. 2) suggests that simple switching between the different connections should provide a plethora of current-time responses that can be useful for preprogramed controlled release and energy conversion.[1,4–6,11–13]

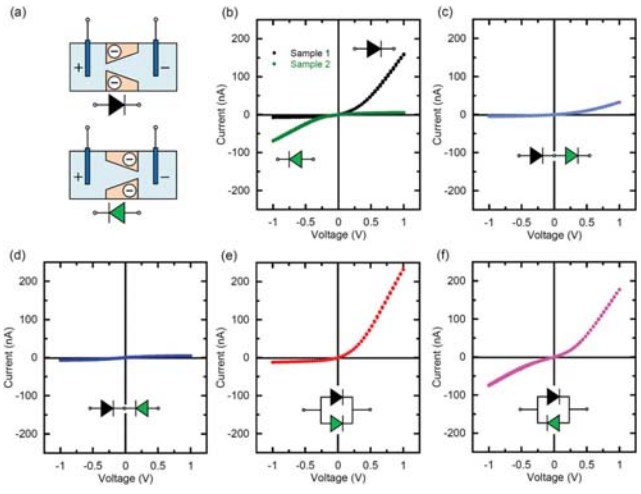

FIG. 1. Experimental I–V curves of the two negatively charged conical nanopores. (a) Schemes of the individual electrochemical cells with samples 1 (upper picture) and 2 (lower picture). (b) I–V curves of samples 1 and 2 with the single nanofluidic diodes in opposite orientations. (c) I–V curve of the series connection with the pores in the same orientation. (d) I–V curve of the series connection with the pores in opposite orientations. (e) I–V curve of the parallel connection with the pores in the same orientation. (f) I–V curve of the parallel connection with the pores in opposite orientations.

The basic applied physics of the nanofluidic diode arrangements can be understood from simple concepts of circuit theory. For instance, Fig. 1(c) shows the total current expected for the diodes in series and their respective individual potential drops, while Fig. 1(e) for the parallel connection shows a total current that is the sum of the individual pore currents. Also, Fig. 1(d) shows the zero current expected from the rectifications of the two pores in series and opposite orientations, while Fig. 1(f) shows two conductive branches because of the opposite pore orientations in the parallel arrangement.

Figures 2(a)–2(c) show the current-time traces for the electrical configurations of Figs. 1(b)–1(f) and three different input potentials $V(t)$.

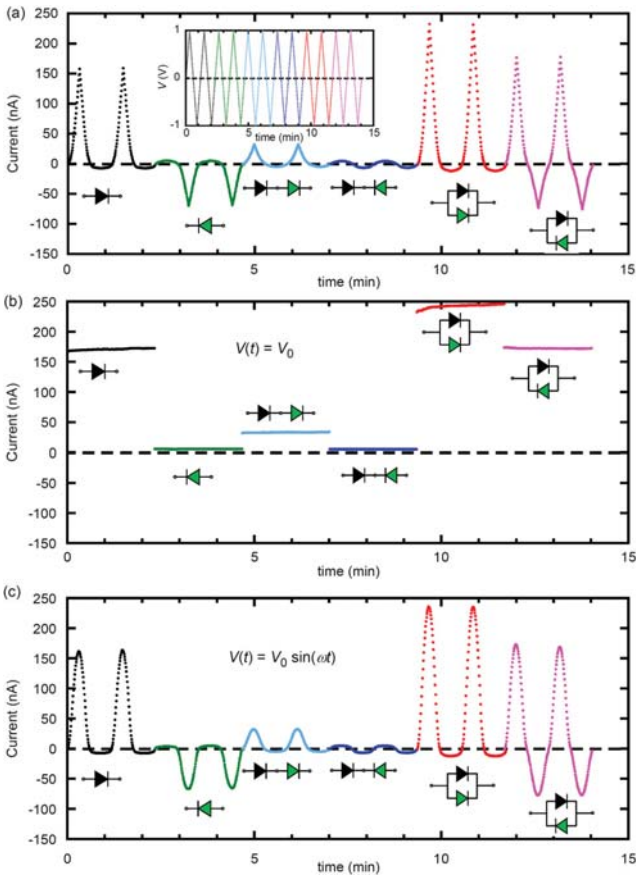

FIG. 2. Current-time (t) traces for the six electrical configurations (*insets*) corresponding to the respective I–V curves of Fig. 1 and three different input potentials $V(t)$. (a) Triangular wave potential. (b) Constant potential. (c) Sinusoidal potential. In all cases, $V_0 = 1$ V and the period $T = 71$ s in cases (a) and (c).

The individual nanopores and the distinct two-pore arrangements respond reliably to triangular wave [Fig. 2(a)], constant [Fig. 2(b)], and sinusoidal [Fig. 2(c)] input potentials, which suggests that preprograming of the desired sequence of switching processes between the different current regimes of Figs. 2(a)–2(c) should be possible. Because the ions and most biomacromolecules present in physiological solutions have net charge, these current regimes should be useful for controlled dispensers based on soft matter nanostructures. In a different but related context, previous experimental work on different nanochannel arrangements has also demonstrated resistive-pulse sensing applications in virus capsids and single macromolecule detection.[14–16]

Note that the system response (current) to the sharp changes in the input signals [voltage peaks in Fig. 2(a)] suggests a reliable switching between other preprogramed sequences. In general, input signals up to 10 – 100 Hz give robust output responses. Also, significant cumulative effects should be possible not only with a constant input potential [Fig. 2(b)] but also with oscillatory signals [Figs. 2(a) and 2(c)] because of the significant rectification observed.

Preprogramed operations and cumulative processes with external white noise signals are interesting in energy conversion and storage. In our case, relevant information on the nanopore performance has been given previously.[13] Figure 3(a) shows the measured current-time traces corresponding to the six electrical configurations of Fig. 1 subjected to a white noise input signal. The cumulative effects are characterized by means of the hybrid electrical circuit of Fig. 3(b) where the nanofluidic diodes are connected with a solid-state charging capacitor. Because of the rectification provided by the different arrangements of nanofluidic diodes, the circuit net current I results in a capacitor voltage V_C after a few minutes in all cases [Fig. 3(c)].

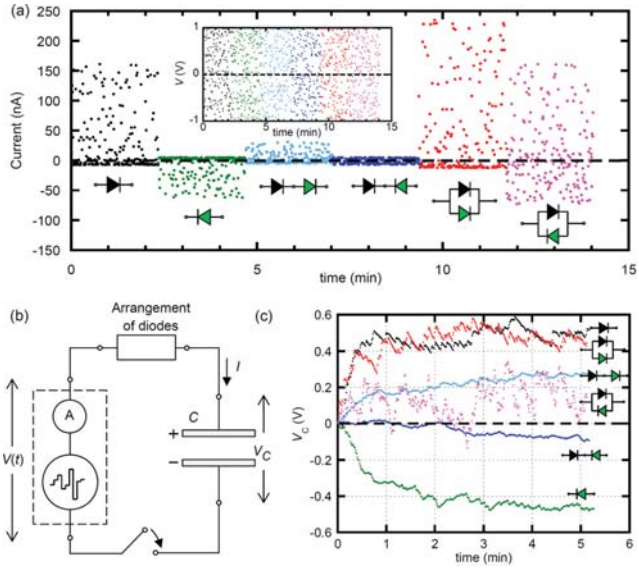

FIG. 3. The cumulative effect achieved with the arrangements of nanofluidic diodes is characterized by the voltage V_C of a capacitor with capacitance $C = 1$ μF. (a) Current-time traces for the six electrical configurations (*bottom insets*) corresponding to the respective I–V curves of Fig. 1 and a white noise input signal $V(t)$ of maximum amplitude $V_0 = 1$ V (*top inset*). (b) Scheme of the electrical circuit with ammeter A controlling the capacitor charging net current I that results from the rectification of $V(t)$ by the different arrangements of diodes. (c) The measured capacitor voltage V_C as a function of time for the six electrical configurations (*insets*).

As expected, the arrangements of Figs. 1(b) and 1(e) give the maximum absolute values of V_C because they show the highest rectification and net current values. In contrast, the series connection of Fig. 1(d) shows only a small (negative) net current I and then a low absolute value of V_C. As to the arrangements of Figs. 1(c) and 1(f), they give intermediate capacitor voltages in Fig. 3(c) because of the moderate net currents. Also, note that the noisy $V_C - t$ traces obtained in the case of the arrangement of Fig. 1(f) result from the relatively high but opposed positive and negative currents in the respective conductive branches, as shown in Fig. 3(a) for this arrangement.

While we have here considered only series and parallel arrangements, mixed series–parallel connections of nanofluidic diodes should also be possible, thus extending the functionality of the proposed conceptual scheme. In principle, the results to be obtained could also be understood by appropriate combinations of the curves obtained in each case using circuit theory concepts. The external regulation of the pore conductance and rectification can also be employed for the implementation of logic functions and information processing in ionic circuits.[2,5,11,17–21] In most applications, undesirable couplings between the electric double layers (EDLs) of adjacent pores can be avoided because the distance between pores is typically much higher than the pore length and much higher than typical EDL thicknesses, which are on the order of a few nanometers for the electrolyte concentrations used here. In this way, our experimental case would correspond to the separation rather than to the synergistic mode because our channel units transport ions independently and the cascade sequence has little effect on response current properties of the system.[22]

In conclusion, we have shown that these nanostructures can be reliably interconnected to increase further their individual functionalities [Figs. 2(a)–2(c)]. In addition, they can be connected with solid-state devices in hybrid circuits [Figs. 3(a)–3(c)] where the liquid-state ionic circuitry can operate similar to traditional solid-state electronic circuits[7,11,13,20] except for the relatively slow time responses which are on the order of 0.1–1 s.[2,13,21] Note that practical applications of these pores in controlled release and energy conversion and storage do not necessarily require fast electrical signals. Because a broad range of surface functionalization and experimental procedures are available to externally modulate the pore charge and conductance,[1,2,4–6,15,17] the single-pore membranes can be employed in electrochemically based energy conversion and storage modules. In the case of controlled release dispensers, however, future work should address the issues of physiological compatibility, device miniaturization, and precise programing of the switching sequences required in each practical application.

Also note that the pores admit different experimental procedures to externally tune the fixed charges of the molecular chains functionalized on the pore surface and could then be used in ionic circuitry with distinct ionic environments.[2] For instance, the monovalent KCl salt can be substituted by the divalent salts $CaCl_2$ and K_2SO_4. The divalent cation Ca^{2+} can be adsorbed on a negative pore, while the divalent anion SO_4^{2-} can be adsorbed on a positive pore, thus reversing the original pore charge in both cases. Therefore, multiple connections of positive and negative pores showing different environmental responses should be obtained. In addition, the experimental behavior obtained previously with a single biological ion channel such as the *OmpF* porin

reconstructed on a lipid bilayer[23] strongly suggests that experimental procedures with artificial biomimetic nanopores could also be extended to arrangements of proteins at the price of a decreased mechanical stability and a more demanding electronics. This fact opens the possibility of using ion channel circuits similar to those used here.

P.R., J.C., V.G., and S.M. acknowledge the funding from Project No. PGC2018-097359-B-100, Spanish Ministry of Science and Education, and FEDER. M.A., S.N., and W.E. acknowledge the support from the LOEWE project iNAPO, Hessen State Ministry of Higher Education, Research and the Arts, Germany. This letter is dedicated to the memory of Professor Julio Pellicer.

REFERENCES

[1]Z. S. Siwy and S. Howorka, Chem. Soc. Rev. **39**, 1115 (2010).
[2]P. Ramirez, J. Cervera, M. Ali, W. Ensinger, and S. Mafe, ChemElectroChem **1**, 698 (2014).
[3]P. Y. Apel, P. Ramirez, I. V. Blonskaya, O. L. Orelovitch, and B. A. Sartowska, Phys. Chem. Chem. Phys. **16**, 15214 (2014).
[4]G. Pérez-Mitta, M. E. Toimil-Molares, C. Trautmann, W. A. Marmisollé, and O. Azzaroni, Adv. Mater. **31**, 1901483 (2019).
[5]H. Zhang, Y. Tian, and L. Jiang, Nano Today **11**, 61 (2016).
[6]M. Tagliazucchi and I. Szleifer, Mater. Today **18**, 131 (2015).
[7]P. Ramirez, V. Garcia-Morales, V. Gomez, M. Ali, S. Nasir, W. Ensinger, and S. Mafe, Phys. Rev. Appl. **7**, 064035 (2017).
[8]P. Apel, Radiat. Meas. **34**, 559 (2001).
[9]Z. Siwy, I. D. Kosińska, A. Fuliński, and C. R. Martin, Phys. Rev. Lett. **94**, 048102 (2005).
[10]J. Cervera, B. Schiedt, R. Neumann, S. Mafe, and P. Ramirez, J. Chem. Phys. **124**, 104706 (2006).
[11]H. Chun and T. D. Chung, Annu. Rev. Anal. Chem. **8**, 441 (2015).
[12]Y. Hou, R. Vidu, and P. Stroeve, Ind. Eng. Chem. Res. **50**, 8954 (2011).
[13]P. Ramirez, J. Cervera, V. Gomez, M. Ali, S. Nasir, W. Ensinger, and S. Mafe, Small **14**, 1702252 (2018).
[14]Z. D. Harms, K. B. Mogensen, P. S. Nunes, K. Zhou, B. W. Hildenbrand, I. Mitra, Z. Tan, A. Zlotnick, J. P. Kutter, and S. C. Jacobson, Anal. Chem. **83**, 9573 (2011).
[15]J. Zhou, P. Kondylis, D. G. Haywood, Z. D. Harms, L. Siang Lee, A. Zlotnick, and S. C. Jacobson, Anal. Chem. **90**, 7267 (2018).
[16]J.-J. Xu, Sci. Bull. **60**, 2067 (2015).
[17]K. Tybrandt, E. O. Gabrielsson, and M. Berggren, J. Am. Chem. Soc. **133**, 10141–10145 (2011).
[18]P. Ramirez, M. Ali, W. Ensinger, and S. Mafe, Appl. Phys. Lett. **101**, 133108 (2012).
[19]X. Duan, T.-M. Fu, J. Liu, and C. M. Lieber, Nano Today **8**, 351 (2013).
[20]J. Cervera, P. Ramirez, V. Gomez, S. Nasir, M. Ali, W. Ensinger, P. Stroeve, and S. Mafe, Appl. Phys. Lett. **108**, 253701 (2016).
[21]V. Gomez, P. Ramirez, J. Cervera, M. Ali, S. Nasir, W. Ensinger, and S. Mafe, Electrochem. Commun. **88**, 52 (2018).
[22]Y. Wang, H. Chen, J. Jiang, J. Zhai, and T. You, ACS Appl. Mater. Interfaces **11**, 26467 (2019).
[23]M. Queralt-Martín, E. García-Giménez, V. M. Aguilella, P. Ramirez, S. Mafe, and A. Alcaraz, Appl. Phys. Lett. **103**, 043707 (2013).